

PROCEEDINGS OF SPIE

[SPIEDigitallibrary.org/conference-proceedings-of-spie](https://spiedigitallibrary.org/conference-proceedings-of-spie)

Time-domain optical coherence tomography can measure artworks with high penetration and high resolution

Bingjie Xu, Kuan He, Pengxiao Hao, Jian Gao, Florian Willomitzer, et al.

Bingjie Xu, Kuan He, Pengxiao Hao, Jian Gao, Florian Willomitzer, Aggelos K. Katsaggelos, John E. Tumblin, Oliver Cossairt, Marc S. Walton, "Time-domain optical coherence tomography can measure artworks with high penetration and high resolution," Proc. SPIE 11058, Optics for Arts, Architecture, and Archaeology VII, 110580M (12 July 2019); doi: 10.1117/12.2525649

SPIE.

Event: SPIE Optical Metrology, 2019, Munich, Germany

Time-domain Optical Coherence Tomography can Measure Artworks with High Penetration and High Resolution

Bingjie Xu^a, Kuan He^a, Pengxiao Hao^b, Jian Gao^a, Florian Willomitzer^a, Aggelos K. Katsaggelos^c, John E. Tumblin^a, Oliver Cossairt^a, and Marc S. Walton^b

^aNorthwestern University, Department of Computer Science, Evanston, IL, USA

^bNorthwestern University, Department of Materials Science & Engineering, Evanston, IL, USA

^cNorthwestern University, Department of Electrical & Computer Engineering, Evanston, IL, USA

ABSTRACT

Accurate measurements of the geometric shape and the internal structure of cultural artifacts are of great importance for the analysis and understanding of artworks such as paintings. Often their complex layers, delicate materials, high value and uniqueness preclude all but the sparsest sample-based measurements (microtomy or embedding of small chips of paint). In the last decade, optical coherence tomography (OCT) has enabled dense point-wise measurements of layered surfaces to create 3D images with axial resolutions at micron scales. Commercial OCT systems at biologically-useful wavelengths (900 nm to 1.3 μ m) can reveal some painting layers, strong scattering and absorption at these wavelengths severely limits the penetration depth. While Fourier-domain methods increase measurement speed and eliminate moving parts, they also reduce signal-to-noise ratios and increase equipment costs. In this paper, we present an improved lower-cost time-domain OCT (TD-OCT) system for deeper, high-resolution 3D imaging of painting layers. Assembled entirely from recently-available commercially-made parts, its 2x2 fused fiber-optic coupler forms an interferometer without a delicate, manually-aligned beam-splitter, its low-cost broadband Q-switched super-continuum laser source supplies 20 KHz 0.4-2.4 μ m coherent pulses that penetrate deeply into the sample matrix, and its single low-cost InGaAs amplified photodetector replaces the sensitive spectroscopic camera required by Fourier domain OCT (FD-OCT) systems. Our fiber and filter choices operate at $2.0 \pm 0.2 \mu$ m wavelengths, as these may later help us characterize scattering and absorption characteristics, and yield axial resolution of about 4.85 μ m, surprisingly close to the theoretical maximum of 4.41 μ m. We show that despite the moving parts that make TD-OCT measurements more time-consuming, replacing the spectroscopic camera required by FD-OCT with a single-pixel detector offers strong advantages. This detector measures interference power at all wavelengths simultaneously, but at a single depth, enabling the system to reach its axial resolution limits by simply using more time to acquire more samples per A-scan. We characterize the system performance using material samples that match real works of art. Our system provides an economical and practical way to improve 3D imaging performance for cultural heritage applications in terms of penetration, resolution, and dynamic range.

Keywords: Optical Coherence Tomography, interferometry, time domain, supercontinuum laser source, pigments

1. INTRODUCTION

Optical Coherence Tomography (OCT) has become attractive in the field of cultural heritage due to its ability to probe the hidden layers of artworks in a non-invasive and non-destructive way.^{1,2} While OCT systems with the central wavelengths from 900 nm to 1.3 μ m are commercially available for biomedical uses, a central wavelength at 2.2 μ m is better suited to detect pigment layers, due to the larger penetration depth.³ Liang *et. al.* have demonstrated that a custom-built 2.2 μ m Fourier domain OCT (FD-OCT) system significantly improved the

Further author information: (Send correspondence to Bingjie Xu)

Bingjie Xu: E-mail: bingjie.xu@u.northwestern.edu

Marc S. Walton: E-mail: marc.walton@northwestern.edu

Optics for Arts, Architecture, and Archaeology VII, edited by Haida Liang,
Roger Groves, Piotr Targowski, Proc. of SPIE Vol. 11058, 110580M
© 2019 SPIE · CCC code: 0277-786X/19/\$21 · doi: 10.1117/12.2525649

imaging depth through oil-paint pigment layers such as titanium white, cobalt blue, and yellow ochre.⁴ However, these FD-OCT systems incorporated a customized high power laser source and a costly broadband spectroscopic camera. To make the system more accessible to a broader user community in the field of cultural heritage, we propose an inexpensive alternative assembled from commercially-available parts; a $2\text{ }\mu\text{m}$ time domain OCT (TD-OCT) system with comparable resolution (axial resolution of $4.85\text{ }\mu\text{m}$), signal quality, and penetration depth. The system reduces cost and equipment complexity substantially, but does require modest increases in measurement time.

Our $2\text{ }\mu\text{m}$ TD-OCT system incorporates a commercial Q-switch supercontinuum source⁵ (power density of 0.04 mW/nm over the wavelength of 1.8 to $2.2\text{ }\mu\text{m}$), a 2×2 fiber coupler, and an InGaAs photodiode detector to reduce the cost. To compensate for the relatively weak laser intensity, we applied a dynamic focus method by using a voice-coil translation stage to move the sample arm, enhancing the interference amplitude and improving the signal-to-noise ratio (SNR). The measurement, control, synchronization, evaluation and display of the data is fully automated in MATLAB, where users can initiate a scanning process performed and completed without any further user guidance.

2. PRINCIPLES

2.1 Time domain OCT (TD-OCT)

OCT systems rely on low-coherence or ‘broadband’ or ‘white-light’ interferometry to precisely compare the lengths of two separate optical paths, as shown in Fig. 1. Similar to a Michelson interferometer, the ‘beam-splitter’ sends light to both the ‘sample arm’ and the ‘reference arm,’ and combines the light that returns from them. Light sent into the ‘reference arm’ reflects from a mirror and returns to the beam-splitter after traversing a path exactly twice as long as the distance to the mirror. Light sent into the ‘sample arm’ illuminates the painting, and each layer of paint may return some light to the beam-splitter by reflection and back-scattering. This small amount of light, which left the beam-splitter and returned by back-scattering from one painting layer, has traversed a path exactly twice as long as the optical distance to the layer (higher index of refraction increases optical distances). If the ‘reference’ and ‘sample’ path lengths match closely (within the coherence length of the light source), resonant wave-fronts combine constructively and destructively at the beam-splitter.

A time-domain OCT system moves the reference-arm mirror to find the distances where interference varies the incident power at its broad-band detector, finding back-scattering depths one-at-a-time. This moving-mirror method may be slow, but applies all available light power to measuring back-scatter of individual, sequential depths. A frequency-domain OCT system keeps its reference mirror fixed during measurements, and replaces the single detector with a spectroscope that measures light power vs. wavelength. The Fourier transform of this measured spectrum then yields a map of all back-scatter strength vs all depths, enabling faster measurements but requiring spectrally-selective detection that must compromise between spectral selectivity, sensitivity, and SNR.

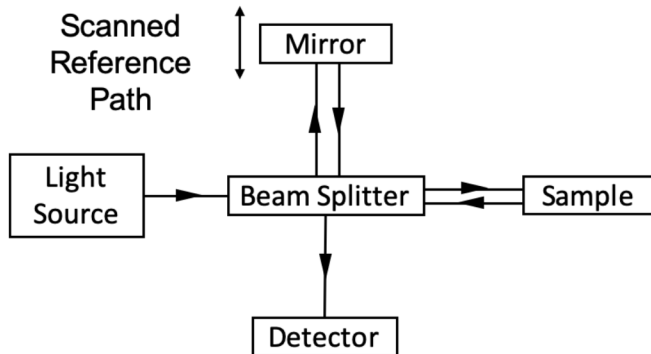


Figure 1. Schematic Diagram of time domain OCT.

2.2 Dynamic focus time domain OCT

In conventional TD-OCT, the reference mirror moves mechanically to generate a depth scan (A-scan). However, when scanning at deeper layers, the coherence gate (the single depth where returned light will cause interference) is out of focus, causing low reflective intensity. It is particularly problematic when using a low-intensity laser, as the interference amplitude may be too small for effective detection. Thus, we devised a dynamic focus TD-OCT setup to increase the reflective intensity which we later found was similar to the method proposed by Hughes *et. al.*⁶ Implementation is simple; instead of moving the reference mirror with the voice-coil translation stage, we keep the mirror fixed and instead move the sample arm assembly, without requiring additional optical parts. By matching the reference path length with the focus point of the scanning lens, the coherence gate remains fixed at or near the beam focus depth throughout the imaging process (Fig. 2a). The different setups for conventional and dynamic focus TD-OCT are shown in Figure 2b.

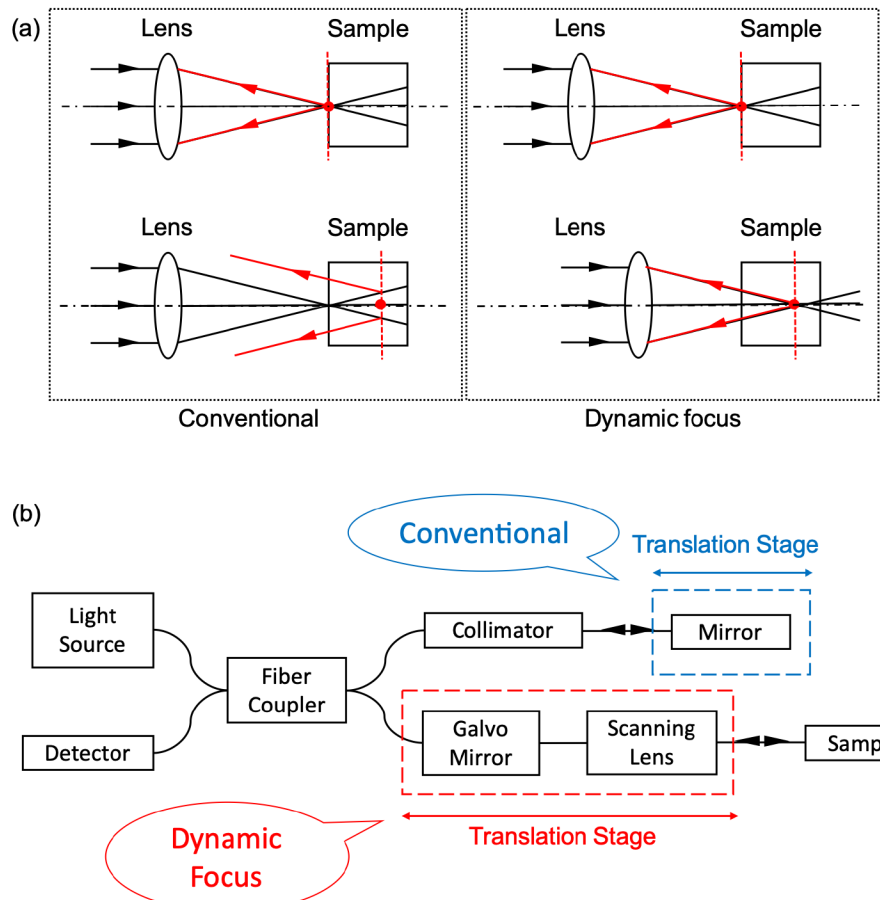


Figure 2. a) Schematic Diagram of light paths in conventional and dynamic focus OCT. The red spot and dashed line represent coherence gate. In conventional OCT, deeper layers will be out of focus and have low reflective intensity. In dynamic focus OCT, layers that match the path-length will be in focus and have high reflective intensity. b) Conventional and dynamic focus OCT apparatus. The blue region depicts conventional OCT, with reference mirror moved by the translation stage; the red region depicts dynamic focus OCT with fixed reference mirror and sample arm moved by the translation stage with galvanometer mirror and scanning lens attached.

3. EXPERIMENTAL METHODS

3.1 The design of the $2 \mu\text{m}$ TD-OCT system

Our OCT system is fiber-based; it replaces the mechanically-vulnerable free-space beam-splitter shown in Figure 1 and is easier to integrate with the near-infrared light source. A low-cost supercontinuum white light laser (NKT SuperK COMPACT) generates light over a wide range, 450-2400 nm, filtered by a bandpass filter (Thorlabs FB2000-500) centered at 2000 nm with 500 nm bandwidth. A collimator couples the free-space light beam source into a 50:50 fiber coupler (2000 ± 200 nm, Thorlabs TW2000R5A2A); the fiber coupler further splits the beam into the reference and sample arms. The scanner on the sample arm consists of a 2D galvanometer system (Thorlabs GVS002) and a scanning lens (Thorlabs SL50-3P) for lateral scan. By putting the scanner on a translation stage (Zaber X-DMQ12P-DE52), the scanning lens can focus at different depths of the sample for the axial scan. The reference arm contains an angular mirror and a neutral density filter to match the beam intensity of the two arms. The fiber coupler further combines the beam from the two arms into the detector (Thorlabs PDA10DT) that records the interference pattern. A multifunction Data Acquisition (DAQ) module (NI USB6003) controls the galvanometer system and captures detector data for use in the MATLAB host computer.

The supercontinuum laser is a pulsed source. Since the time width of each pulse is less than 200 ns, a sampling frequency larger than 10 MHz is necessary to capture each pulse. To decrease the cost of the data acquisition equipment, we use the detector to integrate the signal: the output signal from the detector becomes continuously constant with a bandwidth setting of 500 Hz and a gain setting of 70 dB. This setting enables coherence signal to be obtained without capturing individual pulse peaks by high sample rate data acquisition equipment. Given these parameters, the signal to noise ratio (SNR) is ~ 75 dB with no sample.

In-line on the reference arm, an adjustable neutral density filter helps produce high SNR values, since the amplitude of the interference pattern achieves the maximum when the reflective intensities from the two arms are identical. We also found improvements by using a 3-sided, right-angle corner-reflector or 'retroreflector' as the fixed reference mirror, as it requires little or no alignment with the fiber optic coupler to return maximum light power, and is largely insensitive to environmental vibrations.

On the sample arm, the galvanometer scanning mirrors and the scanning lens are attached to the translation stage. For the following experiment, the lateral resolution of the cross-sectional B-scan is 100 pixels/mm. The velocity of the stage is 1 mm/s; the total scanning depth is 2.5 mm.

A MATLAB application was written for controlling the DAQ and the voice coil stage. The DAQ reads the signal from the detector and generates the analog voltage that controls the galvanometer system. For our TD-OCT system, synchronizing the detector data acquisition with the translation stage positioning commands is critical for capturing well-aligned B-scan data. We found that setting the Windows 10 process priority to its maximum ("real time priority") limited unpredictable delays to < 100 nS and ensured good results.

3.2 Preparation and characterization of the paint layer

Indigo dye ($\text{C}_{16}\text{H}_{10}\text{N}_2\text{O}_2$, KREMER, genuine) and linseed oil (GAMBLIN, cold pressed) were mixed and applied to a microscope slide as a thin layer. After heating the slide at 60°C for one week, the paint layer was dry and freshly characterized using the lab-built $2 \mu\text{m}$ TD-OCT. For comparison, the same slide with paint was characterized by a commercial SD-OCT with a central wavelength at 900 nm (Thorlabs GAN220, bandwidth 150 nm). Additionally, the physical thickness of the paint layer was measured by a Stylus Profilometer (Dektak 150) for ground truth comparison.

4. RESULTS

4.1 Resolution of the $2 \mu\text{m}$ TD-OCT

The fixed but non-Gaussian spectrum of our laser light causes a needlessly broad, non-Gaussian interference pattern at our detector, but we removed this broadening and restored the Gaussian pattern shape by applying the deconvolution method of Bash.⁷ To measure the axial resolution of the $2 \mu\text{m}$ TD-OCT system, we used a microscope glass slide as the sample. The result (Fig. 3) showed that our OCT system achieved a resolution of $\sim 4.85 \mu\text{m}$, comparable to the theoretical resolution ($4.41 \mu\text{m}$).

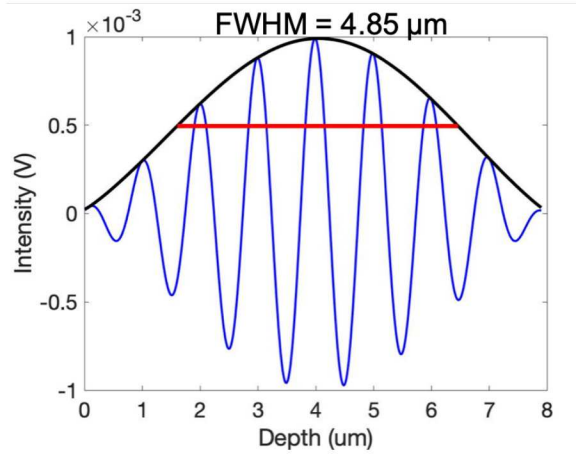


Figure 3. Zoom-in interference pattern at the air/glass interface. The FWHM was $4.85 \mu\text{m}$. The axial resolution of our system achieved a high resolution of $\sim 4.85 \mu\text{m}$ at the air/glass boundary.

4.2 Comparison with the commercial 900 nm FD-OCT

To demonstrate that long wavelength OCT can improve penetration depth, Figure 4 compares the imaging results of our $2 \mu\text{m}$ TD-OCT with a commercial 900 nm FD-OCT for a layer of indigo-linseed-oil on a glass slide. While the indigo layer exhibited strong scattering at 900 nm, as indicated by the absence of the indigo/glass interface, this interface was clear at $2 \mu\text{m}$ (top of Fig. 4a). In addition, the $2 \mu\text{m}$ result revealed the bottom of the glass slide, confirming indigo layer penetration sufficient to measure its underlying layers. The OCT image matched the physical thickness of the indigo layer (Fig. 4c), further validating the result of our $2 \mu\text{m}$ OCT. In addition to indigo, the $2 \mu\text{m}$ laser also proved better penetration ability than the 900 nm laser for several other pigments such as yellow ochre (iron oxyhydroxide) and alizarin crimson (1,2-dihydroxyantraquinone).

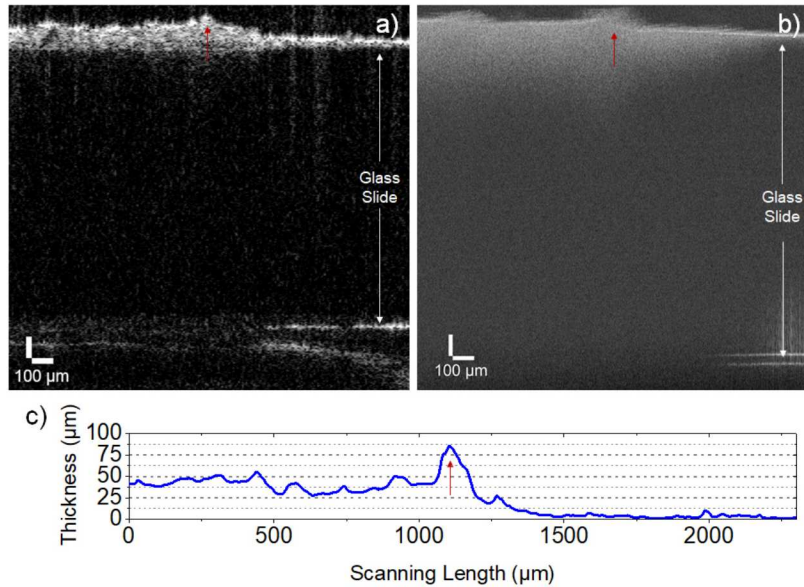


Figure 4. A layer of indigo-linseed-oil on a glass slide scanned by a) lab-built $2 \mu\text{m}$ TD-OCT and b) commercial FD-OCT with a central wavelength of 900 nm . c) The physical thickness of the paint film measured by a profilometer.

5. CONCLUSIONS

We have introduced a dynamic-focus time domain OCT at 2 μm . This OCT system provides resolution and penetration depth suitable for cultural heritage applications. Compared with the commercial OCT systems, a central wavelength at 2 μm improves the depth of penetration for pigments that are opaque in shorter wavelengths. In addition, a broad bandwidth of 400 nm enables an axial resolution of 4.85 μm . Our system applies the dynamic focus setup by placing the translation stage under the galvanometer mirror and scanning lens in the sample arm instead of reference arm. It has greatly improved the system SNR by maintaining the coherence gate near the beam focus throughout the imaging process. All parts in the system are inexpensive off-the-shelf equipment and we provide open source control software.

However, there is still room for further improvement. As we use fibers that do not preserve or maintain the polarization supplied by our laser, better polarization control and matching may further improve system SNR. In addition, the attenuator for matching the intensities of the two arms has been adjusted only at the start of each experiment and kept fixed during measurement, despite weaker signal returns for deeper layers. Dynamically adjusting the attenuator may improve the SNR in the scanning process. Nevertheless, our OCT system is experimentally capable of producing high-resolution high-penetration scanning results of paintings. This simple and inexpensive OCT system can be widely used in cultural heritage area. Moreover, the scanning results of our system will be fused with pigment identification methods in further studies.

ACKNOWLEDGMENTS

This project is partially funded by Northwestern University's Center for Scientific Studies in the Arts, made possible by generous support of the Andrew W. Mellon Foundation (20182023). Additional funding from NSF PIRE (#1743748): Computationally-Based Imaging of Structure in Materials (CuBISM) is gratefully acknowledged. This work made use of the Keck-II facility of Northwestern University's NUANCE Center, which has received support from the Soft and Hybrid Nanotechnology Experimental (SHyNE) Resource (NSF ECCS-1542205); the MRSEC program (NSF DMR-1720139) at the Materials Research Center; the International Institute for Nanotechnology (IIN); the Keck Foundation; and the State of Illinois, through the IIN.

REFERENCES

- [1] Drexler, W. and Fujimoto, J. G., *[Optical coherence tomography: technology and applications]*, Springer Science & Business Media (2008).
- [2] Stifter, D., "Beyond biomedicine: a review of alternative applications and developments for optical coherence tomography," *Applied Physics B* **88**, 337–357 (2007).
- [3] Liang, H., Lange, R., Peric, B., and Spring, M., "Optimum spectral window for imaging of art with optical coherence tomography," *Applied Physics B* **111**(4), 589–602 (2013).
- [4] Liang, H., Cheung, C. S., Daniel, J. M. O., Tokurakawa, M., Clarkson, W. A., and Spring, M., "High resolution fourier domain optical coherence tomography at 2 microns for painted objects," in *[Optics for Arts, Architecture, and Archaeology V]*, *Proc. SPIE* **9527**, 952705 (2015).
- [5] Maria, M., Gonzalo, I. B., Feuchter, T., Denninger, M., Moselund, P. M., Leick, L., Bang, O., and Podoleanu, A., "Q-switch-pumped supercontinuum for ultra-high resolution optical coherence tomography," *Optics Letters* **42**(22), 4744 (2017).
- [6] Hughes, M. and Podoleanu, A. G., "Simplified dynamic focus method for time domain oct," *Electronics Letters* **45**(12), 623–624 (2009).
- [7] Bashkansky, M., Duncan, M., Reintjes, J., and Battle, P., "Signal processing for improving field cross-correlation function in optical coherence tomography," *Appl. Opt.* **37**, 8137–8138 (1998).